Optics Communications 443 (2019) 150–155

Contents lists available at ScienceDirect

Optics Communications

journal homepage: www.elsevier.com/locate/optcom

High-power single-longitudinal-mode double-tapered gain-coupled distributed feedback semiconductor lasers based on periodic anodes defined by i-line lithography

Yuxin Lei [a,b], Yongyi Chen [a,*], Feng Gao [a], Dezheng Ma [a,b], Peng Jia [a], Hao Wu [a], Chao Chen [a], Lei Liang [a], Jun Zhang [a], Jingyu Tian [a,b], Li Qin [a], Yongqiang Ning [a], Lijun Wang [a]

[a] State Key Laboratory of Luminescence and Application, Changchun Institute of Optics, Fine Mechanics and Physics, Chinese Academy of Sciences, Changchun 130033, China
[b] University of Chinese Academy of Sciences, Beijing 100049, China

ARTICLE INFO

Keywords:
Semiconductor lasers
Distributed feedback lasers
Gain-coupled
Double-tapered

ABSTRACT

In this paper, we demonstrate a regrowth-free double-tapered gain-coupled distributed feedback semiconductor laser. It is designed based on periodic surface current injection to reach a high-power and single-longitudinal mode. A continuous-wave output power of over 1.2 W/facet is achieved at 4 A. High single-longitudinal-mode output power reaches up to 0.9 W/facet at 3 A at each uncoated facet. The side mode suppression ratio is nearly 30 dB at 980 nm. The 3 dB spectral width is less than 2.7 pm. The lateral far field divergence angle is only 14.5°, the beam quality factor M^2 is 1.7, achieving a near-diffraction-limit emission. Our device, produced by standard i-line lithography, enhances the output power while obtaining the pleasurable spectral and spatial properties. It has great potential in widespread commercial applications such as high efficiency pumping sources for its low-cost, easy fabrication technique and excellent performance.

1. Introduction

High power, single-longitudinal-mode (SLM) and narrow-linewidth semiconductor lasers with compact sizes and long lives are desirable for numerous traditional applications, such as high efficiency pumping sources for fiber amplifiers [1] used in telecommunication systems [2], or solid-state lasers used in material processing [3]. It is also highly demanded in other application areas that expanding with the development of the artificial intelligence, such as sensing [4], scanning [5–7], and measurement [8]. The master oscillator power amplifier (MOPA) structure is widely used to amplify the output power without degeneration in beam quality [9]. Over the past decades, monolithically integrated MOPA laser devices have been greatly developed. Different approaches have been applied to improve the electrical, spectral, spatial and thermal characteristics of MOPA laser devices [10–14]. Most of them consist of a ridge waveguide and a tapered waveguide. The ridge waveguide is usually either a Distributed Bragg Reflector (DBR) [10,11] or a Distributed Feedback (DFB) [12] laser, such as the 12 W high-brightness single-frequency DBR tapered diode laser [10], the 5 W DBR tapered lasers emitting at 1060 nm with a narrow spectral linewidth and a near-diffraction-limit beam quality [11], and the 973 nm DFB MOPA device with a continuous wave (CW) output power of 3.7 W [12].

In this paper, we propose a double-tapered gain-coupled DFB laser based on periodic current injection. The device achieves high SLM output power and excellent beam quality while the fabrication steps and costs are significantly reduced. Gain contrasts in quantum wells are achieved by periodic current injection from periodic surface metal p-contacts insulated with periodic shallow-etched grooves. The grooves were fabricated only by conventional micron-scale i-line lithography technology and dry ion etching technology without high-cost, complicated and time-consuming processing steps such as nanometer-scale lithography or secondary epitaxy growth. High power in SLM operation is achieved by introducing the MOPA structure, which consists of a ridge waveguide with 44th-order gain-coupled grooves and two symmetrical tapered waveguides. The CW output power at 4 A is up to 1.2 W/facet, the CW output power in SLM operation is up to 0.9 W/facet at 3 A. The maximum side mode suppression ratio (SMSR) is nearly 30 dB at 980 nm, and the 3 dB spectral width is less than 2.7 pm. The lateral far field divergence angle is only 14.5°, the beam quality factor M^2 is 1.7, achieving a near-diffraction-limit emission. Our double-tapered gain-coupled DFB laser requires a simple processing technique which is compatible with existing fabrication techniques of the conventional semiconductor lasers. Due to the easy fabrication technique and excellent performance, our device provides a novel method

* Corresponding author.
E-mail addresses: chenyy@ciomp.ac.cn (Y. Chen), summit1990@163.com (F. Gao), jiapeng@ciomp.ac.cn (P. Jia).

https://doi.org/10.1016/j.optcom.2019.02.073
Received 30 November 2018; Received in revised form 20 February 2019; Accepted 25 February 2019
Available online 14 March 2019
0030-4018/

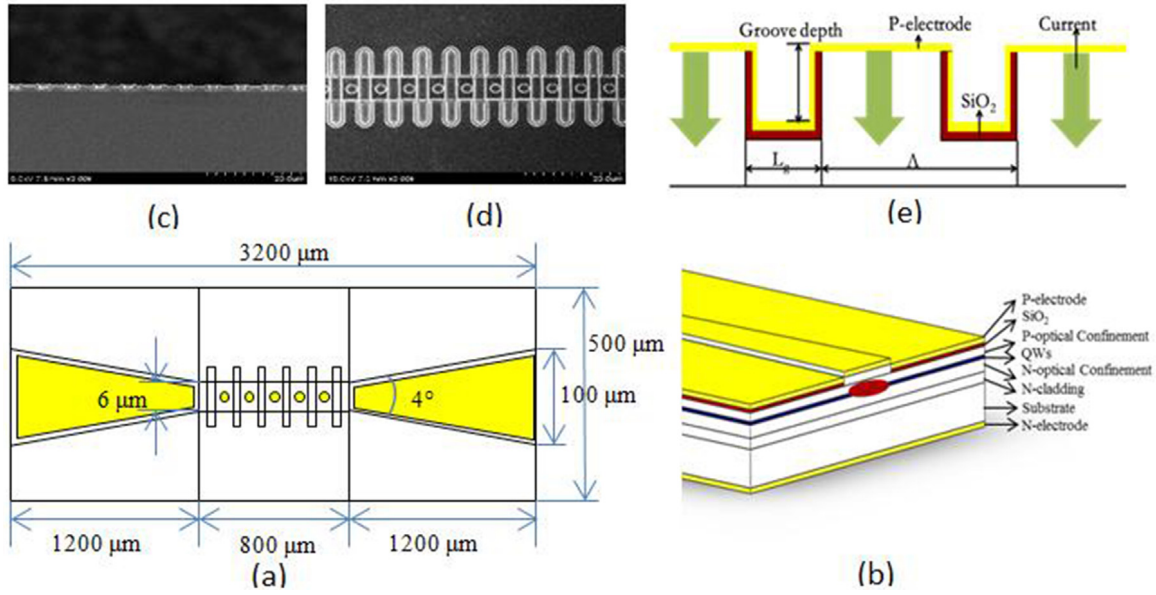

Fig. 1. The schematic diagram of the double-tapered gain-coupled DFB laser device. (a) Layout of the double-tapered gain-coupled DFB laser with periodic electrodes. (b) Epitaxial layer structure. (c) The scanning electron microscope image of the periodic surface electrodes from lateral view. (d) The scanning electron microscope image of the periodic surface etched grooves from top view. (e) Periodic current injection schematic.

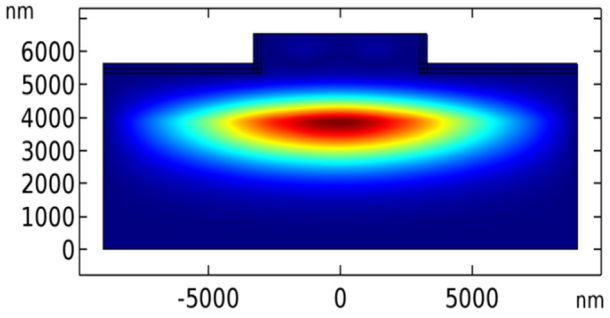

Fig. 2. The optical field distribution of the ridge waveguide with the width of 6 μm and the etching depth of 1.2 μm.

to fabricate practical high-power high-beam-quality gain-coupled DFB laser for widespread commercial applications.

In the following sections, we present the design process and the performance of our device. First, a brief overview of the device structure is given. Second, the details of design and fabrication are presented. Finally, the results regarding electro-optical, spectral and spatial properties of our device are provided.

2. Device structure design and fabrication

The schematic diagram of the double-tapered gain-coupled DFB diode laser is shown in Fig. 1. As Fig. 1(a) shows, the device consists of a 6 μm-wide, 800 μm-long ridge waveguide with 44th order surface-etched gain-coupled grooves and two symmetrical 1200 μm-long index-guided tapered waveguides listed on both sides of the ridge waveguide separately. The width of the tapered waveguide is increased linearly from 6 μm to 100 μm with a full tapered angle of 4°. The epitaxial layer structure is shown in Fig. 1(b). A self-designed ultra-low-aluminum asymmetric ultra-large-optical-cavity (ULOC) separate confinement heterostructure (SCH) with double strain-compensated InGaAs quantum wells [13] is used to reach high output power and to reduce catastrophic optical damage (COD).

The ridge waveguide listed in the middle of the device serves as a modal filter to simultaneously achieve fundamental transverse mode [13] and SLM emission. The width and etching depth of the ridge waveguide are determined by the combination of the theory and experimental conditions in order to achieve fundamental transverse mode emission at high power [14,15]. The width of the ridge waveguide is set to be 6 μm to achieve fundamental transverse mode operation through diffraction effect [16]. The etching depth is determined in consideration of the balance between the effective optical field restriction and the minimum optical field loss. The single mode operation is achieved with the width of 6 μm and the etching depth of 1.2 μm as the corresponding fundamental-transverse-mode optical field distribution calculated by the commercial software COMSOL Multiphysics shown in Fig. 2.

The SLM operation benefits from the additional wavelength selective feedback of the gain-coupled grooves on the ridge waveguide. The gain-coupled mechanism is formed by periodic current injection from periodic surface metal p-contacts and insulated periodic shallow-etched surface grooves filled with silica as the schematic shown in Fig. 1(e). The insulated grooves can effectively increase the gain contrast in the quantum wells [17]. The gain-coupled grooves modulate the imaginary part of the coupled coefficient [18], the coupling coefficient κ of our gain-coupled DFB device is $\kappa = i\frac{\Delta g \Gamma}{4}$, where Δg is the gain/loss contrast in the waveguide, and Γ is the optical confinement factor in the quantum wells. As it can be seen from the formula, κ is independent of grooves' period, we use micron-scale high-order grooves to achieve gain-coupled mechanism and reduce the processing difficulty. And as the scanning electron microscope (SEM) image shown in Fig. 1(c), the surface etched grooves are modeled in the shape of rectangle, and the length of each groove is 2 μm, which is compatible with our alignment technology in the fabrication. The etching depth of surface grooves is designed to enhance gain contrast in the quantum wells without introducing effective index-coupled effect, and the etching depth is finally set to be 0.7 μm according to the optical field distribution in [17]. The coupling strength of our gain-coupled DFB on the ridge waveguide is 0.0337. The micron-scale grooves are not as precise as nanometer-scale grating [15], or as complicated as apodized grating [19], they only require standard i-line lithography and ordinary ion etching with high reproducibility. In comparison with electron-beam lithography, the i-line lithography is more practical and applicable in actual production to achieve structures with low costs and simplified manufacturing processes. Then, the high-order shallow-etched gain-coupled grooves periodically modulate the gain

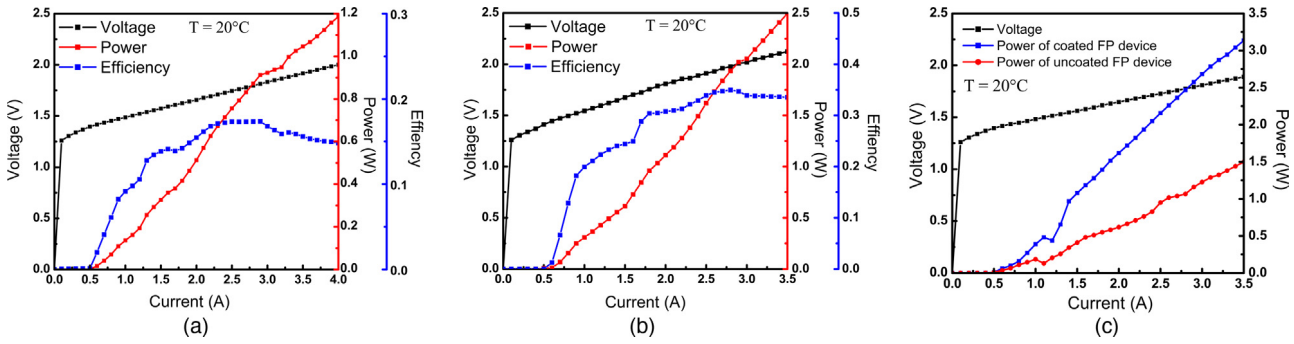

Fig. 3. Measured power–current–voltage characteristics and electro-optical efficiency profiles of (a) uncoated and (b) coated double-tapered gain-coupled DFB laser device, and (c) the comparison of power–current characteristics between coated and uncoated FP laser devices.

distribution and achieve a SLM narrowband emission with a simple fabrication technique.

The periodic surface etched grooves are shown from top view in the SEM image in Fig. 1(d), the width of the grooves is 20 μm. The grooves are wider than the ridge waveguide. The excess parts aside the ridge waveguide serve as beam spoilers. They are used to filter the backward propagating field out of the ridge waveguide and help maintain stable fundamental transverse mode operation [20]. The nonlinear effects, such as longitudinal spatial hole burning (LSHB) and filament effect, are also suppressed [16]. Though the losses to the fundamental mode and the high-order transverse modes would be simultaneously introduced, simulations were carried out by COMSOL Multiphysics about the energy ratio in beam spoilers of fundamental mode (TE_{00}) and first-order mode (TE_{01}). The results show that the optical energy distributed in the grooves is only 0.790% of the total TE_{00} optical mode field energy. The ratio of the TE_{01} mode is 1.762%, which is about 1.2 times higher than that of the fundamental mode. In other words, the grooves introduce much more losses to high-order transverse modes than to the fundamental mode. What is more, traditional beam spoilers require one or more additional separate processing steps [16,20], the spoilers of our device are simultaneously formed with the gain-coupled grating without other complicated processes, the technique is simplified and the technological tolerance is increased at the same time.

Double tapered waveguides are utilized for optical amplification to enhance the output power in SLM operation and superior beam quality [14,21]. The gradually varied width of the tapered waveguide provides more scattering losses to high-order transverse modes than to fundamental transverse mode during transmission [15]. The full tapered angle of double tapered waveguides is chosen to be 4° due to the fundamental mode diffraction full angle at $1/e^2$ [22] to prevent high-order transverse modes coupling into the ridge waveguide. The lengths of the ridge waveguide and double tapered waveguides are derived from the balance of the mode filtering and power amplification. Longer ridge waveguide would provide much more effective mode filtering with the sacrifice of output power. Longer tapered waveguides would provide a larger current injection area resulting in greater power amplification but unstable mode operation. And the length of the tapered waveguides further relates to the surface area of the output facets. The width of the output facet determines the width of the aperture, and further influences the far field patterns and the difficulties of coupling and shaping. Finally, the lengths of the ridge waveguide and double tapered waveguides are set to be 800 μm and 1200 μm. Furthermore, the nonlinear effects, such as LSHB and filament effect, caused by self-focusing effect are effectively avoided by drastically reducing the peak intensity of light propagation field [16]. Meanwhile, the levels of the COD at both rear and front facets are effectively improved by remarkably increasing the surface areas of facets, the power density at facets are significantly reduced [23]. And the maximum output power is improved. In addition, the index-guided tapered waveguides are adopted for more effective photon restriction than the gain-guided tapered waveguides, thus the slow axis far-field divergence angle of our device is dramatically reduced. The index-guided tapered waveguides could be formed simultaneously with the ridge waveguide, the fabrication process is simplified as well. Hence, our double tapered waveguides provide the power amplification with a simple fabrication technique but no degradation of fundamental transverse mode operation.

The epitaxial layer structure was grown by metal organic chemical vapor deposition (MOCVD) on a GaAs substrate. After the epitaxial material growth, the device structure was precisely defined and formed by standard i-line lithography technique and inductively coupled plasma (ICP) dry etching. The surface grooves were formed in waveguide layer, the lateral waveguide was practically etched to waveguide layer. After that, chips with periodic surface metal p-electrode, which covered with electroplated gold, were cleaved into bars with a cavity length of 3.2 mm after metallization. The bars were then cleaved into single laser emitters and were packaged p-side down on sub-mounts with hard solder. Golden wire bonding was used to achieve effective electrical connection between n-side and sub-mount. Then, the chips on sub-mounts were mounted on copper heat sinks with water-cooling for further test and analysis. The double-tapered gain-coupled DFB laser device and the reference Fabry–Perot (FP) laser device in the following experiment section were fabricated simultaneously from the same wafer. And the FP laser device share the identical structure with the DFB laser device only with the exception of the shallow-etched surface grooves.

3. Experiment results and discussion

All measurements of the experiment were carried out under CW conditions at a heat sink temperature of 20 °C. The optical output power was measured with a thermoelectric detector, which was calibrated as national standards, placed directly in front of the output facet. The optical spectrum was measured directly by coupling the laser with a 10 μm core diameter fiber-linking YOKOGAWA AQ6370C optical spectrum analyzer. It was checked that the measured spectra, especially the peak positions, were not affected by the position of the fiber, and the results were reproducible. The spectral width was measured by coupling the collimating laser to Fabry–Perot Interferometer (FPI) (Thorlabs, SA200-8B) with a resolution of 67 MHz and a free spectral range of 10 GHz. The beam waist width was measured after collimation with a fast axis collimating lens, a slow axis collimating lens and a focusing lens.

The power–current–voltage (P–I–V) characteristics and electro-optical efficiency profiles of the uncoated and coated 3.2 mm-cavity-length double-tapered gain-coupled DFB laser devices are shown in Fig. 3(a) and (b). The P–I–V characteristics of the uncoated and coated FP laser devices are shown in Fig. 3(c) for comparison. The threshold currents of all four devices are around 0.5 A. The optical output power of the gain-coupled DFB laser device increases almost linearly until an

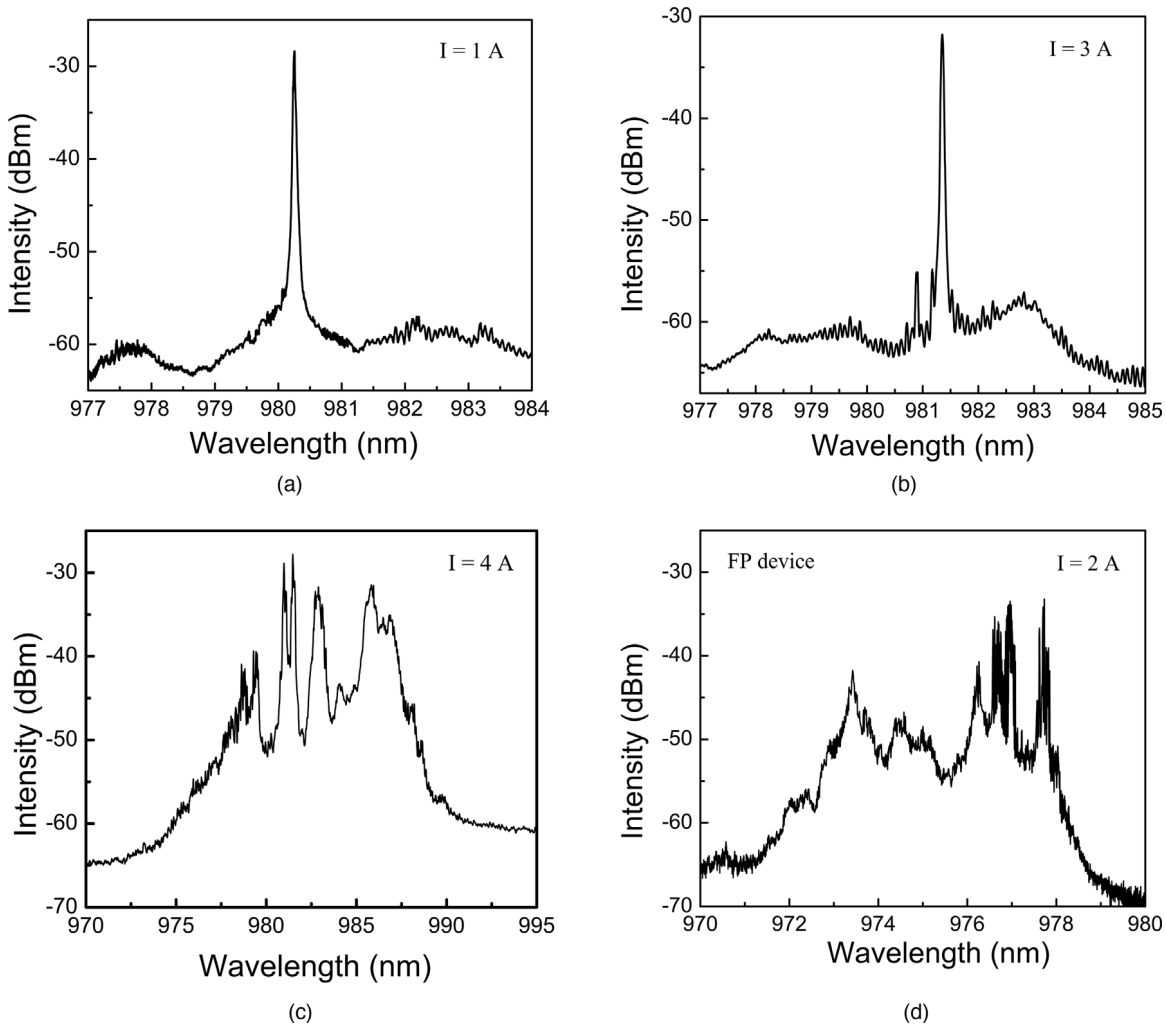

Fig. 4. The optical spectra of the double-tapered gain-coupled DFB laser device at (a) 1 A (b) 3 A (c) 4 A and the FP laser device at (d) 2 A.

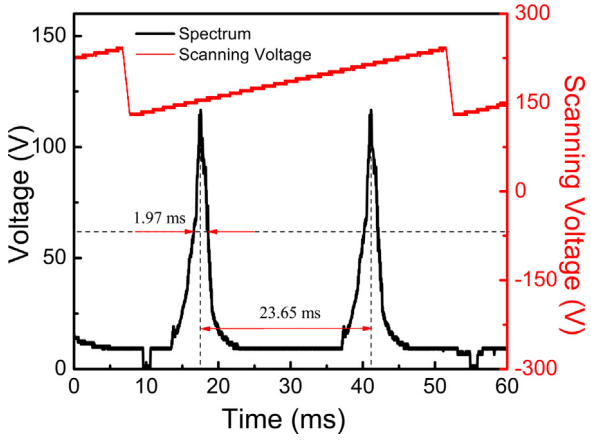

Fig. 5. The spectral width pattern of the coated double-tapered gain-coupled DFB laser device at 0.8 A.

injection current of 4 A without roll-over or COD. The output power is up to 1.2 W/facet at 4 A, the slope efficiency is about 0.34 W/A, much larger than the published MOPA laser device with the slope efficiency of 0.23 W/A [15]. The electro-optical efficiencies were calculated from the P–I–V characteristics. The maximum electro-optical efficiency is up to 18% at an output power of 0.73 W/facet. After coating with anti-reflectivity and high-reflectivity films on front and rear facets respectively, the output power is enhanced to 2.5 W at 3.5 A, the slope efficiency is enhanced to 0.83 W/A, and the maximum electro-optical efficiency is significantly enhanced to 35% at 1.65 W.

The optical spectra of the double-tapered gain-coupled DFB laser device and FP laser device are shown in Fig. 4. As shown in Fig. 4(a) and (b). The DFB laser device keeps on-axis main-lobe emission and operates in SLM even at high currents, the maximum CW output power of the uncoated device in SLM operation is up to 0.9 W/facet at 3 A, which is much larger than our previously reported SLM DFB laser with the SLM output power of 48.8 mW/facet [17]. As shown in Fig. 4(c), multiple-longitudinal-mode operation appears when the current rises beyond 3 A. That is the main reason leading to the kink at around 3 A of the P–I curve of gain-coupled DFB laser device. The mode degradation at higher currents is potentially caused by the mode competition (or multimode effect) and temperature rise within the device. The main reason causing the modal instabilities is the coupling between the ridge waveguide and the tapered waveguide, leading to the nonlinear of the P–I characteristic [16]. It should be mentioned that the slope efficiency and the output power of the gain-coupled DFB laser device are both inferior to the FP laser device, but the FP laser device shows a kink at even lower current around 1 A due to the complex multiple modes in the cavity as shown in Fig. 4(d). The maximum SMSR of the gain-coupled DFB laser device is nearly 30 dB at around 980 nm at 1.1 A, which is much larger than previously published double-tapered laser device with the SMSR of 27 dB [15]. As shown in Fig. 5, the measured 3 dB spectral width of the narrowband single emission is less than 2.7

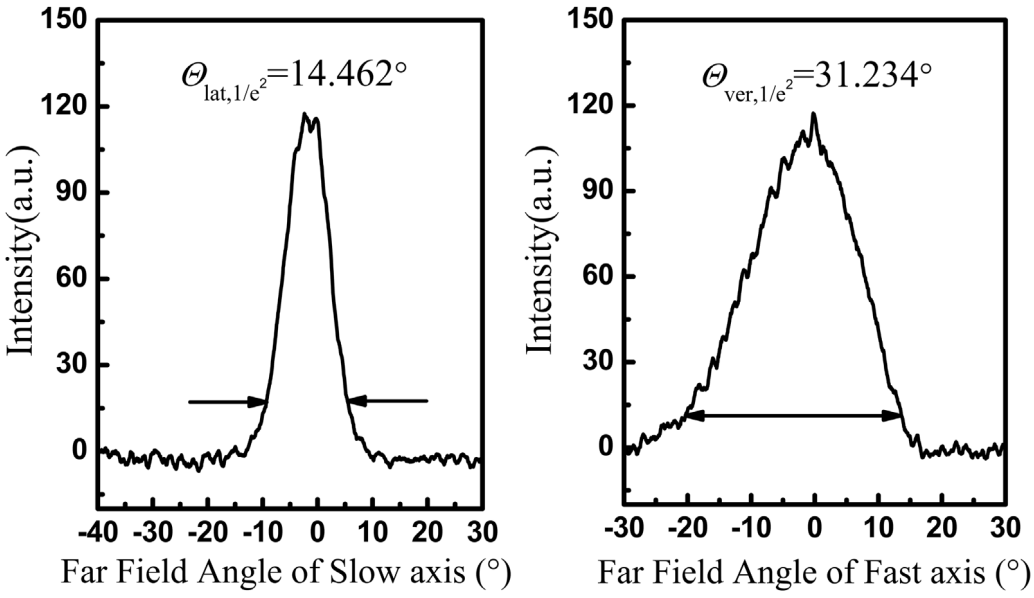

Fig. 6. The lateral/vertical far field patterns of the gain-coupled DFB laser device at 3 A.

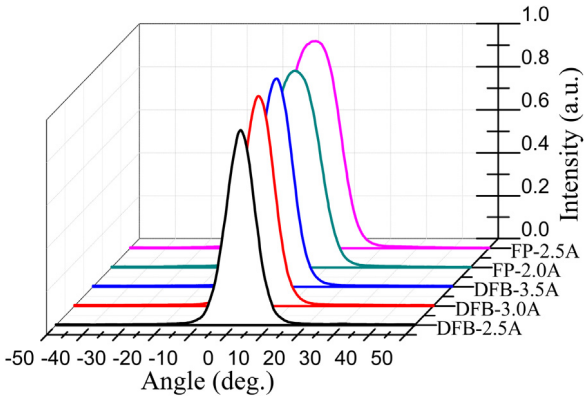

Fig. 7. Normalized intensity distributions of the lateral far field patterns of the DFB and FP laser device at different currents.

pm, which is much narrower than the previously reported DFB laser with the spectral width of 3.2 pm [17].

The lateral and vertical far-field patterns of the gain-coupled DFB laser device at 3 A are depicted in Fig. 6. Due to the implementing of an asymmetric large optical cavity with the active layer positioned not in the middle of the waveguide layers but closer to the p-side, the far-field beam divergence angle in fast axis at $1/e^2$ is about 31.23°. And the far-field beam divergence angle in slow axis at $1/e^2$ is only 14.46°. For the tapered waveguide leads to an optical beam with strong astigmatism [16,20,24,25], the beam waist width at virtual source position is measured to be 8.65 μm after collimation, and the beam propagation ratio is M^2 = 1.7 ($1/e^2$ level). An excellent near-diffraction-limit beam quality is achieved. Normalized intensity distributions of the lateral far field patterns of DFB and FP laser device are shown in Fig. 7, from threshold to 3.5 A, the lateral far-field beam divergence angles at $1/e^2$ are all below 15° with similar shapes. And the lateral far-field beam divergence angle of the DFB laser device is 7.5° smaller than FP laser device at the same current of 2.5 A. Our device with such stable characteristics at high output powers is extremely attractive for mass production, and is highly desirable for widespread commercial applications.

4. Conclusion

In summary, we have presented a regrowth-free double-tapered gain-coupled DFB semiconductor laser with high-order surface-etched gain-coupled grooves based on periodic current injection. It only requires simple micron-scale fabrication technique by standard i-line lithography, and provides CW output power of 1.2 W/facet at 4 A. Measured output power at 3 A is up to 0.9 W/facet in SLM operation. The SMSR is nearly 30 dB at 980 nm, and 3 dB spectral width is less than 2.7 pm. The excellent near-diffraction-limit beam quality is achieved with M^2 of 1.7. Due to the excellent electro-optical, spectral and spatial properties, our device provides highly desirable potential utilized value in more commercial application areas of low-cost mass production.

Acknowledgments

This work was supported by National Science and Technology Major Project of China (2016YFE0126800); Frontier Science Key Program of the President of the Chinese Academy of Sciences, China (QYZDY-SSW-JSC006); National Natural Science Foundation of China (NSFC) (11874353, 61727822, 61674148, 11604328, 51672264, 61474117, 61874119); Natural Science Foundation of Jilin Province (Jilin Province Natural Science Foundation), China (20160520017JH, 20170623024TC); Opened Fund of the State Key Laboratory of Integrated Optoelectronics, China No. IOSKL2018KF21; Science and Technology Key Project of Jilin Province, China (20170204013GX); Science and Technology Development Project of Jilin Province, China under Grant (20180201014GX).

References

[1] R. Paschotta, J. Nilsson, A.C. Tropper, D.C. Hanna, Ytterbium-doped fiber amplifiers, IEEE J. Quantum Electron. 33 (1997) 1049–1056.
[2] L. Greusard, D. Costantini, Near-field analysis of metallic DFB lasers at telecom wavelengths, Opt. Express 21 (2013) 10422–10429.
[3] W. Schulz, R. Poprawe, Manufacturing with novel high-power diode lasers, IEEE J. Quantum Electron. 6 (2000) 696–705.
[4] J.J. Coleman, A.C. Bryce, C. Jagadish, Advances in Semiconductor Lasers, 2012.
[5] A.R. Nehrir, K.S. Repasky, J.L. Carlsten, Eye-safe diode-laser-based micropulse differential absorption lidar (DIAL) for water vapor profiling in the lower troposphere, J. Atmos. Ocean. Technol. 28 (2011) 131–147.
[6] B.W. Tilma, M. Mangold, C.A. Zaugg, S.M. Link, D. Waldburger, A. Klenner, A.S. Mayer, E. Gini, M. Golling, U. Keller, Recent advances in ultrafast semiconductor disk lasers, Light Sci. Appl. 4 (2015) e310.

[7] E.C. Burrows, K.Y. Liou, High resolution laser LIDAR utilising two-section distributed feedback semiconductor laser as a coherent source, Electron. Lett. 26 (1990) 577–579.
[8] H. Peng, Y. Wang, Dynamic time-correlated single-photon counting laser ranging, Optoelectron. Lett. 2 (2018) 129–132.
[9] M. Vilera, A. Pérez-Serrano, J.M.G. Tijero, I. Esquivias, Emission characteristics of a 1.5 um all semiconductor tapered master oscillator power amplifier, IEEE Photonics J. 7 (2) (2015) 1500709.
[10] C. Fiebig, G. Blume, C. Kaspari, D. Feise, J. Fricke, M. Matalla, H. Wenzel, K. Paschke, G. Erbert, 12W High-brightness single-frequency DBR tapered diode laser, Electron. Lett. 44 (21) (2008) 1253–1255.
[11] K.-H. Hasler, B. Sumpf, P. Adamiec, F. Bugge, J. Fricke, P. Ressel, H. Wenzel, G. Erbert, G. Trankle, 5-W DBR Tapered lasers emitting at 1060 nm with a narrow spectral linewidth and a nearly diffraction-limited beam quality, IEEE Photonics Technol. Lett. 20 (19) (2008) 1648–1650.
[12] M. Spreemann, M. Lichtner, M. Radziunas, U. Bandelow, H. Wenzel, Measurement and simulation of distributed feedback tapered master-oscillator power-amplifiers, IEEE J. Quantum Electron. 45 (6) (2009) 609–616.
[13] Y. Chen, P. Jia, J. Zhang, L. Qin, Gain-coupled distributed feedback laser based on periodic surface anode canals, Appl. Opt. 54 (2015) 8863–8866.
[14] S.F. Yu, Double-tapered-waveguide distributed feedback lasers for high-power single-mode operation, IEEE J. Quantum Electron. 33 (1997) 71–80.
[15] L. Liu, H. Qu, High-brightness single-mode double-tapered laser diodes with laterally coupled high-order surface grating, Opt. Lett. 39 (2014) 3231–3234.
[16] M. Mikulla, Tapered high-power high-brightness diode lasers: design and performance, Top. Appl. Phys. 78 (2000) 265–288.
[17] F. Gao, L. Qin, Y. Chen, Study of gain-coupled distributed feedback laser based on high order surface gain-coupled gratings, Opt. Commun. 410 (2018) 936–940.
[18] A. Orth, J.P. Reithmaier, R. Zeh, First order gain-coupled GaInAs/GaAs distributed feedback laser diodes patterned by focused ion beam implantation, Appl. Phys. Lett. 69 (1996) 1906–1908.
[19] Y. Shi, S. Li, R. Guo, R. Liu, Y. Zhou, X. Chen, A novel concavely apodized DFB semiconductor laser using common holographic exposure, Opt. Express 21 (2013) 16022–16028.
[20] I. Esquivias, A. Perez-Serrano, J.M.G. Tijero, High-brightness tapered lasers. chap. 28 of handbook of optoelectronic device modeling and simulation, in: J. Piprek (Ed.), Lasers, Photodetectors, Solar Cells, Novel Applications, and Mathematical Methods, vol. 2, Taylor & Francis, Boca Raton, FL, ISBN: 9781498749565, 2017.
[21] J.N. Walpole, Semiconductor amplifiers and lasers with tapered gain regions, Opt. Quantum Electron. 28 (1996) 623–645.
[22] A. Müller, J. Fricke, F. Bugge, O. Brox, G. Erbert, B. Sumpf, DBR Tapered diode laser with 127 W output power and nearly diffraction-limited, narrowband emission at 1030 nm, Appl. Phys. B 122 (2016) 87.
[23] J.S. Yoo, H.H. Lee, P. Zory, Temperature rise at mirror facet of CW semiconductor lasers, IEEE J. Quantum Electron. 21 (1985) 1913–1918.
[24] H. Wenzel, B. Sumpf, G. Erbert, High-brightness diode lasers, C. R. Phys. 4 (6) (2003) 649–661.
[25] B. Sumpf, K.-H. Hasler, P. Adamiec, F. Bugge, F. Dittmar, J. Fricke, H. Wenzel, M. Zorn, G. Erbert, G. Trankle, High-brightness quantum well tapered lasers, IEEE J. Sel. Top Quantum Electron. 15 (3) (2009) 1009–1020.